Linear Spectral Mixture Analysis Based Approach with Regard to Neighboring Pixels for Multispectral Image Classification

Nareenart Raksuntorn
Faculty of Industrial Technology, Suan Sunandha Rajabhat University, Thailand
E-mail: nareenart@ssru.ac.th

and **Winai Raksuntorn**
Faculty of Engineering, Thammasat University, Thailand
E-mail: rwinai@engr.tu.ac.th

Manuscript received October 17, 2015
Revised November 16, 2015

ABSTRACT

This paper presents an algorithm to implement a linear spectral mixture analysis (LSMA) based approach with regard to neighboring pixels for multispectral image classification. This approach allows the implementation of LSMA in the way of the traditional manner does, i.e., an unconstrained LSMA (ULSMA). In our approach, a given pixel and its neighboring pixels are involved in the unmixing process. A given pixel will be classified as a material corresponding to the maximum abundance if the resulting abundances are all non-negative. Otherwise, the algorithm goes to a searching process. In this process, the algorithm searches for abundances obtained from a given pixel and its neighboring pixels that are satisfied three conditions: non-negativity, sum-to-one, and minimum mean squares error on reflectance reconstruction (MSER). Here, the endmember sets used in the searching step are varied where endmembers corresponding to nonnegative numbers are fixed and other endmembers can be varied. Five experiments for a real multispectral image are conducted including an ULSMA, a multiple endmember spectral mixture analysis (MESMA), the proposed approach with one-pixel and two-pixel distances, and a maximum likelihood (ML) estimation. The first three methods are based on the LSMA method while the last one, ML, is based on parameter estimation. Three major material types: water, vegetation, and road/building, are present in the image scene. The experimental results demonstrated that the proposed method offered higher classification accuracy when compared to the ULSMA and MESMA. The overall accuracies were about 89.50% and 88.50% for one-pixel and two-pixel distances, respectively. However, when compared to the ML classifier, the proposed approach provided a lower accuracy in overall. Specifically, the proposed approach yielded higher accuracies for two classes: water and vegetation. But for the road/building class, the performance of the proposed approach was lower due to endmember variability. When compare the computational cost, the proposed approach outperformed both MESMA and ML.

Keywords: *Multispectral image; classification; linear spectral mixture analysis*

1. INTRODUCTION

Recently, remote sensing data have been the principal earth observing and monitoring and they are become increasing available. Two major types of remote sensing data include hyperspectral and multispectral images. Hyperspectral images consist of hundreds of sensors operating at contiguous spectral ranges for capturing images while multispectral images have a small number of sensors and only several spectral bands are available. Due to their coarse spatial resolution, a pixel is actually mixed by materials present in the image scene and such pixel is called a mixed pixel. In some cases, a pixel may cover by only one material and this pixel is defined as a pure pixel or called an endmember signature. Therefore, the same material will have the same distinct spectral signature. In multispectral image analysis, we are most interested in land cover or land

used. Therefore, a mixed-pixel will be identified as a specific cover material. Also, in traditional image analysis each pixel will be classified without regard to neighboring pixels.

Linear spectral mixture analysis (LSMA) has been widely used and succeeds in many applications for multispectral images [1] – [3]. It requires only a *prior* knowledge about the number of materials and their types present in the image scene. LSMA can be applied for sub-pixel or mixed-pixel classifications. Least squares (LS) method is a commonly used approach for LSMA. For a sub-pixel classification, it is to estimate all proportions of materials present in a given pixel. In the other hand, for a mixed-pixel classification, a given pixel is labeled as a single material. For a mixed-pixel classification, LSMA processes two sequential steps: estimate abundances (linear spectral unmixing) and classify the mixed-pixel. In the first step, LSMA is used to estimate the abundances or proportions of materials present in a given pixel. And in the second step, the given pixel will be classified according to the estimated abundances. Since the resulting abundances are proportions of materials in the image scene, the given pixel will be identified as a single material assumed to be present the dominant material within a pixel, i.e., the material corresponding to the maximum abundance. To estimate abundances, LSMA models a pixel reflectance as a linear combination of endmember signatures and their corresponding abundances. Due to mathematical calculations, the resulting abundances may be negative values or greater than one. To obtain physical meaning of abundances, two constraints must be imposed, i.e., sum-to-one and non-negativity [4]. However, forcing the constraints may lead inaccurate results. A multiple endmember spectral mixture analysis (MESMA) was developed to relax the two constraints by allowing the number of endmembers and their types to be varied from pixel to pixel [5]. In the conventional MESMA, endmember signatures used in the mixture model are obtained from the spectral library. Hence, MESMA suffers from a problem in practice since it has an excessive computational cost caused by the number of pairs to be searched. In addition, a small threshold must be predefined for non-negative abundances. Later, an endmember-variable LMM (EVLMM) was developed. It was original proposed for searching an actual endmember set (AES) for a given pixel of hyperspectral images [6]. EVLMM does not require any preset threshold because it searches for the endmember set from all the endmembers present in the image scene where the resulting abundances are automatically sum-to-one and non-negativity. In fact, EVLMM still has an exhausting searching style because it searches for a combination of endmembers that produces all non-negative abundances. If the interested image scene is highly mixed, EVLMM is not preferred.

Herein, we proposed an implementation of LSMA based approach with regard to neighboring pixels for multispectral image classification. Since it is obvious that a small neighborhood tends to have a similar set of materials, it may be useful to add neighboring pixels into a mixture model of LSMA to improve the classification result. So, in our approach, not only a given pixel is involved in the mixture model, but also the neighboring pixels as adopted by the idea from [7]. The implementation step is similar to the unconstrained LSMA (ULSMA), i.e., abundances are estimated by LS and no constraints are imposed. Materials corresponding to negative abundances are most likely not present in a pixel; therefore, those materials are removed from the mixture model. Then the remaining materials are assumed to be the AES. Applying the AES in the mixture model, the pixel that produces all abundances satisfied the three conditions: non-negativity, abundance sum, and MSER, will be selected. Then the given pixel will be classified as a material that corresponding to the maximum abundances obtained from the selected pixel. By these ways, it can improve the classification accuracy and may reduce computational times compare to the conventional LSMA and MESMA.

The remainder of this paper is organized as follows. Section 2 describes related work including both LSMA and MESMA. Section 3 introduces the proposed approach. Section 4 conducts the experiments. Finally, section 5 summarizes the contributions of this paper.

2. RELATED WORK

2.1. LSMA

In LSMA, a pixel is described as a linear combination of endmember signatures and their abundances as follows.

$$\mathbf{r} = \mathbf{M}\boldsymbol{\alpha} + \mathbf{n}, \tag{1}$$

where $\mathbf{r}$ is $L \times 1$ column pixel vector with L being the number of spectral bands, $\mathbf{M} = [\mathbf{m}_1, \mathbf{m}_2, \ldots, \mathbf{m}_p]$ is the endmember signature matrix containing p endmembers, $\boldsymbol{\alpha} = (\alpha_1, \alpha_2, \ldots, \alpha_p)^T$ is the abundance vector with α_j being the abundance fraction of $\mathbf{m}_j$ present in $\mathbf{r}$, and $\mathbf{n}$ is an additive noise. When the number of endmembers and their signatures are known, LS approach can be used to estimate the abundances such that the pixel reconstruction error is minimized, i.e.,

$$\min_{\hat{\alpha}} \|\mathbf{r} - \mathbf{M}\hat{\boldsymbol{\alpha}}\|^2. \tag{2}$$

The solution of Eq. (2) can be expressed by

$$\hat{\boldsymbol{\alpha}} = \left(\mathbf{M}^{\mathrm{T}}\mathbf{M}\right)^{-1}\mathbf{M}^{\mathrm{T}}\mathbf{r}. \quad (3)$$

It is noted that the estimated abundances solved by Eq. (3) can be non-negative values due to mathematical calculation. In this paper, LSMA is referred to as the ULSMA, where only a given pixel is considered and there is no constraint.

2.2. MESMA

In this paper, MESMA is referred to as the EVLMM. This algorithm assumes that there is an optimal endmember set for a given pixel. Using the optimal endmember set to estimate abundances, the resulting should be automatically sum-to-one and non-negativity, i.e.,

$$\sum_{j=1}^{p} \alpha_j = 1 \text{ and } \alpha_j \geq 0. \quad (4)$$

In general, MSER depends on the number of endmembers; the larger the number of endmembers, the smaller MSER. So, the algorithm will search for the combination with fewer endmembers that produces all nonnegative abundances with the smallest MSER. For each pixel, the algorithm steps can be described as follows [6].

1. Normalize pixel vectors and all the endmember signatures to ensure that the abundances obtained from the LS are not dominated by their high energies, to which the MSER is sensitive. For example, if a less-significant endmember with a higher energy is removed from the endmember set, the corresponding MSER may be larger, which introduces an inaccurate endmember set.

2. Set the image endmember set as the initial endmember set (IES) then determine the abundances using the IES with the LS. If the abundances are all nonnegative values, the IES is kept as the AES. If one or more negative abundances are obtained, go to the next step.

3. Find the abundances from the combinations with one endmember, apply the LS, and then calculate the MSER. Keep the combination that produces all nonnegative abundances with the minimum MSER.

4. Repeat Step 3 by searching from the two-endmember combinations. If the minimum MSER in the current step is greater than that in the previous step, the combination obtained from the previous step is selected as the AES and the algorithm is terminated. Otherwise, test the combinations with more endmembers.

3. PROPOSED APPROACH

In this section, we present an algorithm for multispectral image classification using the LSMA based approach with regard to neighboring pixels. The proposed approach searching steps are based on the three conditions including: 1) a given pixel and its neighboring pixels are included in the mixture model, 2) the materials corresponding to negative abundances are considered to be removed from the mixture model, and 3) using the remaining materials, the classification result will be from the pixel generating all non-negative abundances that are satisfied sum-to-one and the minimum MSER. For a given pixel, the implementation steps of our approach shown in Fig. 1 can be described as follows.

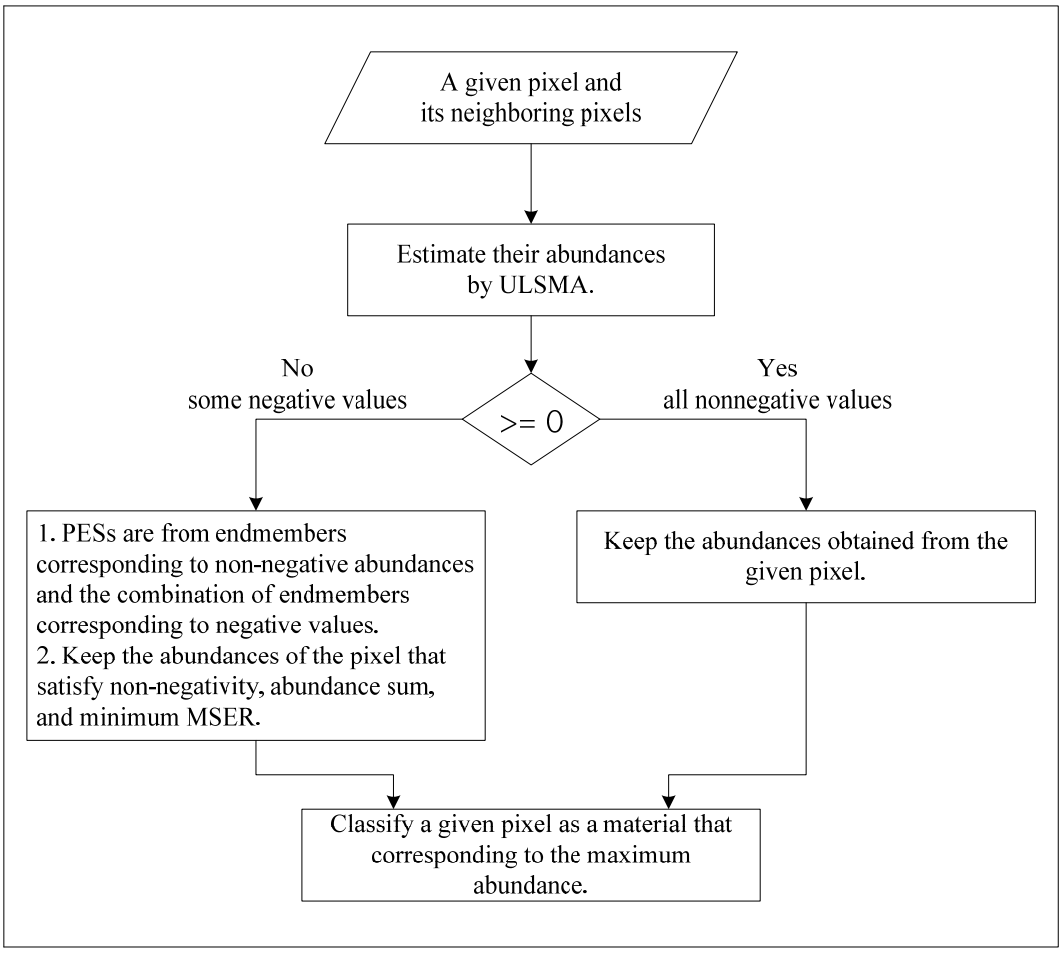

Fig. 1 *Block diagram of the proposed approach.*

1. Identify neighboring pixels. In this paper, one-pixel and two-pixel distances are considered, where a one-pixel distance contains 4 neighboring pixels and a two-pixel distance includes 8 neighboring pixels. Fig. 2 illustrates a given pixel and its neighboring pixels, where X represents a given pixel and Y1 - Y8 represent neighboring pixels.

2. Set the image endmember set as the IES then apply ULSMA to estimate abundances of the given pixel and its neighboring pixels.

3. Consider the resulting abundances. If abundances obtained from the given pixel are all nonnegative, keep these abundances and go to Step 4. Otherwise, remove endmember(s) that corresponding to negative abundances from the mixture model and re-estimate all pixels' abundances using the remaining endmembers. At this stage, if there are two or more endmembers to be removed, the searching step will be similar to that of the MESMA. Hence, the possible endmember sets (PESs) to be searched are chosen based on the abundance sign: the endmembers corresponding to nonnegative abundances are fixed and the other can be varied. Keep the abundances of the pixel that satisfy non-negativity, abundance sum, and minimum MSER.

4. Classify the given pixel as a material that corresponding to the maximum abundance obtained from Step 3.

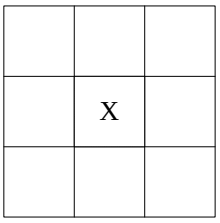

(a) a given pixel

Fig. 2 *A given pixel and its neighboring pixels. (cont.)*

	Y1	
Y2	X	Y3
	Y4	

(b) a one-pixel distance.

Y5	Y1	Y6
Y2	X	Y3
Y7	Y4	Y8

(c) a two-pixel distance.

Fig. 2 *A given pixel and its neighboring pixel.s*

4. EXPERIMENTS

A multispectral image used in this study was taken by World-View 2 cover the area of Dusit District, Bangkok, Thailand, with a size of 250×250×8 pixels. The spatial resolution is about 1.84 m. This image was recorded in January 2010. Fig. 3 (a) shows the 8^{th} band. The color image, where vegetation is green, is shown in Fig. 3(b).

(a) band 8

Fig. 3 *A multispectral image scene used in the experiment. (cont.)*

(b) color image

Fig. 3 *A multispectral image scene used in the experiment.*

Dusit area is located about the center of Bangkok. This area comprises a lot of human made such as constructions. There are 3 major materials present in the image scene including water, vegetation, and road/building. Although the image spatial resolution is quite high compared with other multispectral data, the samples used in the experiment are actually not pure. Firstly, they are randomly selected throughout from the image scene based on their ground truth. Since Dusit is a density district, it includes several different construction types, some human made, water areas and vegetation. Some materials may even cover a small area. Secondly, samples are involved with two conditions: atmospheric such as moisture and cloud, and the surrounding materials such as shading and shadows. The later condition often occurs in the urban.

Five experiments were conducted to compare their classification results. These experiments are to examine the classification results of ULSMA, MESMA, ML, and the proposed approach using 4 and 8 neighboring pixels. It is noted that ULSMA, MESMA, and the proposed approach are based on the LSMA algorithm while the ML is based on parameter estimation. The ML is also a common and widely used algorithm for remote sensing data classification. In this paper, the ML was implemented as a supervised method, where it requires training samples and their labels. In the other hand, the ULSMA, MESMA, and the proposed approach were implemented as a semi-supervised method, where only endmember signatures are known. In some practices, ML may not be applicable since training samples are quite limited and their quality may be poor.

There are 250 samples for each material. 50 samples of each material were averaged and used for class endmember for ULSMA, MESMA, and the proposed approach. These 50 samples were used as training samples for the ML as well. The remaining samples were used for testing validation. Tables 1 - 5 list the overall accuracies, kappa coefficients, producer's accuracies and errors of omission, user's accuracies and errors of commission produced by ULSMA, MESMA, ML, and the proposed approach with 4 and 8 neighboring pixels, respectively.

Table 1 *ULSMA classification result.*

Classification results	References			total of row	User's accuracy (%)	Error of commission (%)
	water	vegetation	road/building			
water	199	1	78	278	199/278 = 71.58	28.42
vegetation	1	181	1	183	181/183 = 98.91	1.09
road/building	0	18	121	139	121/139 = 87.05	12.95
total of column	200	200	200	600		
Producer's accuracy (%)	199/200 = 99.50	181/200 = 90.50	121/200 = 60.50	overall accuracy = (199+181+121)/600 = 83.50%		
Error of omission (%)	0.50	9.50	39.50	kappa coefficient = 0.75		

Table 2 *MESMA classification result.*

Classification results	References			total of row	User's accuracy (%)	Error of commission (%)
	water	vegetation	road/building			
water	199	1	78	278	199/278 = 71.58	28.42
vegetation	1	188	1	190	188/190 = 98.95	1.05
road/building	0	11	121	132	121/132 = 90.91	9.09
total of column	200	200	200	600		
Producer's accuracy (%)	199/200 = 99.50	188/200 = 94.00	121/200 = 60.50	overall accuracy = (199+188+121)/600 = 84.67%		
Error of omission (%)	0.50	6.00	39.50	kappa coefficient = 0.77		

Table 3 *ML result.*

Classification results	References			total of row	User's accuracy (%)	Error of commission (%)
	water	vegetation	road/building			
water	193	8	5	206	93.69	6.31
vegetation	6	183	6	195	93.85	6.15
road/building	1	9	189	199	94.97	5.03
total of column	200	200	200	600		
Producer's accuracy (%)	193/200 = 96.50	183/200 = 91.50	189/200 = 94.50	overall accuracy = (193+183+189)/600 = 94.17%		
Error of omission (%)	3.50	8.50	5.50	kappa coefficient = 0.91		

Table 4 *The proposed approach with 4 neighboring pixels classification result.*

Classification results	References			total of row	User's accuracy (%)	Error of commission (%)
	water	vegetation	road/building			
water	199	1	45	245	199/245 = 81.22	18.78
vegetation	1	185	2	188	185/188 = 98.40	1.60
road/building	0	14	153	167	153/167 = 91.62	8.38
total of column	200	200	200	600		
Producer's accuracy (%)	199/200 = 99.50	185/200 = 92.50	153/200 = 76.50	overall accuracy = (199+185+153)/600 = 89.50%		
Error of omission (%)	0.50	7.50	23.50	kappa coefficient = 0.84		

Table 5 *The proposed approach with 8 neighboring pixels classification result.*

Classification results	References			total of row	User's accuracy (%)	Error of commission (%)
	water	vegetation	road/building			
water	199	1	50	250	79.60	20.40
vegetation	1	184	2	187	98.40	1.60
road/building	0	15	148	163	90.80	9.20
total of column	200	200	200	600		
Producer's accuracy (%)	199/200 = 99.50	184/200 = 92	148/200 = 74	overall accuracy = (199+184+148)/600 = 88.50%		
Error of omission (%)	0.50	8	26	kappa coefficient = 0.83		

From the classification results, it can be seen that the overall accuracies produced by ULSMA, MESMA, ML, and the proposed method with 4 and 8 neighboring pixels were 83.50% with kappa coefficient 0.75, 84.67% with kappa coefficient 0.77, 94.17% with kappa coefficient 0.91, 89.50% with kappa coefficient 0.84, and 88.50% with kappa coefficient 0.83, respectively. Over all, the ML yielded the most accuracy and kappa coefficient. However, when compare individual class accuracy, all methods based on LSMA approach produced the highest accuracy of water while the ML offered the minimum accuracy. This may be from water signatures are quite different from the other two classes, and most spectral signatures of water are similar. For vegetation, all methods provided similar results; the accuracies were about 90.50% - 94%. This is because spectral signatures of vegetation are similar. When consider road/building, only ML generated good results while the results from LSMA-based classifiers were poor. The ML produced an accuracy of 94.50%. The results of LSMA-based approaches were about 60.50%, 60.50%, 76.50%, and 74% for ULSMA, MESMA, and the proposed method with 4 and 8 neighboring pixels, respectively. Road/building samples are from different types of materials such as concrete, metal, wood, and asphalt. So, these samples are quite different and some of them may be similar to other classes as we can see from the results that the confusions between road/building and water were high for all cases. Many road/building samples were identified as water with error of commission about 19% - 28%. Thus, linear regression does not work well when endmember are variability. Among the LSMA-based approaches, the proposed approach with 4 neighboring pixels could outperform. In fact, adding all the neighboring pixels may not be useful as we can see that when 8 neighboring pixels were added, the accuracy was lower. The reason for this is that not all the neighboring pixels are similar, especially in the border area. To enhance the classification accuracy, one might select only neighboring pixels that are similar to the given pixel. The ULSMA yielded the worst performance since its abundances were not realistic.

To compare their computational costs, we recorded the run time of each experiment. All experiments were run by the same personal computer (PC) with 1.6 GHz CPU and 2 GB memory. The run times are shown in Table 6. From the results, we can see that MESMA took 54.26 seconds; ML consumed 36.54 seconds; the proposed approach with 4 neighboring pixels spent only 35.89 seconds; the proposed approach with 8 neighboring pixels required 41.08 seconds. It can be seen that ULSMA is the most fastest since there is no constraint. The run time of the proposed method with 4 neighboring pixels is the minimum. It is noted that the run time of the proposed approach increases as the number of neighboring pixels increase.

***Table 6** The computational time.*

Methods	Computational time (s)
ULSMA	0.07
MESMA	54.26
ML	36.54
proposed approach with 4 neighboring pixels	35.89
proposed approach with 8 neighboring pixels	41.08

5. CONCLUSIONS

In this paper, we have proposed an algorithm for multispectral image classification using the LSMA based approach with regard to neighboring pixels. In the proposed approach, spatial neighbors are added into the mixture model to improve the classification accuracy as it is assumed that a pixel and its neighbors generally comprise the similar materials. First, the proposed algorithm estimates abundances for all the pixels and then removes the endmembers corresponding to the negative abundances. Only endmembers produce non-negative abundances will be used to re-calculate the abundances for the next step. Then the classification result will be from the pixel resulting in all non-negative abundances that are satisfied sum-to-one with the minimum MSER. Experimental results show that the proposed approach yields higher classification accuracy with a lower the computational cost compared to other LSMA-based approaches. When compare the proposed method's performance to the ML, the overall accuracy and kappa coefficient of the proposed method are lower; the accuracy of road/building is lower but the accuracies of water and vegetation are higher. This is because the LSMA-based approach is sensitive to endmember variability while the performance of ML depends on the number of training samples and their quality. The future work may work on the selection of neighboring pixels since all of the 4 or 8 neighboring pixels may not consist of the similar materials as the given pixel. Methods for selecting neighboring pixels may include spectral angle mapper (SAM) or spatial homogeneity index introduced by [8].

6. ACKNOWLEDGEMENTS

This research was supported in part by Suan Sunandha Rajabhat University.

REFERENCES

[1] M. T. Mayes, J. F. Mustard, and J. M. Melillo, "Forest cover change in Miombo woodlands: modeling land cover of African dry tropical forests with linear spectral mixture analysis," *Remote Sensing of Environment*, vol. 165, pp. 203-215, 2015.

[2] D. Sun and N. Liu, "Coupling spectral unmixing and multiseasonal remote sensing for temperate dryland land-use/land-cover mapping in Minqin County, China," *International Journal of remote sensing*, vol. 36, pp. 3636-3658, 2015.

[3] C. W, C. Deng and X. Jai, "Spatially constranied multiple endmember spectral mixture analysis for quantifying subpixel urban impervious surfaces," *IEEE Journal of Selected Topics in Applied Earth Observations and Remote Sensing*, vol.7, no. 6, pp.1976-1984, 2014.

[4] Y. E. Shimabukuro and J. A. Smith, "The least-squares mixing models generate fraction images derived from remote sensing multispectral data," *IEEE Transaction on Geoscience Remote Sensing*, vol. 29, no. 1, pp. 16-20, 1991.

[5] D. A. Roberts, M. Gardner, R. Church, S. Ustin, G. Scheer, and R. O. Green, "Mapping chaparral in the Santa Monica Mountains using multiple endmember spectral mixture models," *Remote Sensing Environment*, vol. 38, no. 2, pp. 267-279,1998.

[6] N. Raksuntorn and Q. Du, "A new linear mixture model for hyperspectral image analysis," *Proceedings of IEEE Geoscience and Remote Sensing Symposium*, 3, pp. 258-261, 2008.

[7] Y. Chen, N. M. Nasrabadi, and T. D. Tran, "Hyperspectral image classification using dictionary-based sparse representation," *IEEE Transaction on Geoscience Remote Sensing*, vol. 49, no. 10, pp. 3973- 3985, 2011.

[8] G. Martin and A. Plaza, "Spatial-Spectral Preprocessing prior to endmember identification and unmixing of remotely sensed hyperspectral data," *IEEE Journal of Selected Topics in Applied Earth Observations and Remote Sensing*, vol.5, no. 2, pp.380-395, 2012.

Nareenart Raksuntorn received the Ph.D. degree in Electrical Engineering from Mississippi State University in 2009. She is currently an assistant professor in the Faculty of Industrial Technology at Suan Sunandha Rajabhat University. Her research interests include remote sensing, image processing, and pattern recognition.

Winai Raksuntorn received the Ph.D. degree in Civil Engineering from University of Colorado in 2002. He is currently an assistant professor in the Faculty of Engineering at Thammasat University. His research interests include pavement design, transportation engineering, and surveying engineering.